Letters

Accurate SM Disturbance Observer-Based Demagnetization Fault Diagnosis With Parameter Mismatch Impacts Eliminated for IPM Motors

Yaofei Han, *Member, IEEE*, Shaofeng Chen, *Student Member, IEEE*, Chao Gong, *Member, IEEE*, Xing Zhao, *Member, IEEE*, Fanggang Zhang, and Yunwei Li, *Fellow, IEEE*

***Abstract*—This letter proposes a novel sliding mode (SM) disturbance observer-based technique to diagnose demagnetization fault of interior permanent magnet (IPM) motors with stator parameter mismatch impacts eliminated. First, the IPM motor model incorporating the disturbances caused by the PM demagnetization and stator parameter mismatch is established. Then, an SM disturbance observer is constructed to identify the overall disturbance caused by all parameters, with its stability discussed by using the Lyapunov function. Third, a current-analysis-based method is developed to extract the disturbance only caused by flux linkage mismatch from the overall disturbance. Third, the extracted disturbance is adopted to calculate the real flux linkage, achieving demagnetization fault judgment and demagnetization degree calculation. Finally, experiment is conducted on two IPM motors to validate the proposed flux linkage estimation and fault diagnosis methods.**

***Index Terms*—Demagnetization fault diagnosis, disturbance, interior permanent magnet (IPM) motor, parameter mismatch, sliding mode (SM) observer.**

I. Introduction

INTERIOR permanent magnet (IPM) motors are characterized by high-power density, high efficiency, and compact structure, thereby being widely adopted in electric vehicles, high-speed railways, and home appliances [1]. However, in comparison with the traditional induction motors, permanent magnets (PMs) that are inclined to get demagnetized in harsh environments (e.g., high temperature and intensive vibration) need to be installed in the rotor of an IPM motor. In practice, once the demagnetization fault occurs, both stator currents and torque ripples will increase, reducing the system performance as well as the reliability [2]. On this ground, it is valuable to diagnose the demagnetization fault timely so as to issue a necessary alert for IPM motor maintenance or replacement.

Many up-to-date studies have developed demagnetization diagnosis techniques for the IPM motors, which can be categorized into offline strategies and online strategies [3], [4], [5], [6], [7], [8], [9], [10], [11], [12]. In terms of the offline strategies, they are achieved by comparing the back electromotive force (EMF) variations before and after the fault occurs [3], [4]. However, the back EMF can only be accurately detected when the machine works as a generator, it is not convenient to apply the offline strategies to the in-service motors. As for the online strategies, they can be divided into three groups based on the signals used for analysis: stator-current-based method [5], magnetic-signal-based method [6], [7], [8], [9], [10] and mechanical-signal-based method [11], [12]. Among these methods, the magnetic-signal-based method is the most direct way to diagnose the demagnetization fault because either the flux density or flux linkage is adopted for analysis [13]. And one typical case is flux linkage observer-based diagnosis scheme. In 2012, patent US20120074879 A utilized a magnetic flux observer to estimate the real-time flux linkage [6], which can be employed to determine whether a motor experiences the demagnetization fault by comparing the estimated flux linkage with the preliminarily set value (healthy motor's flux linkage). Afterward, varieties of flux linkage observers have been developed, including extended Kalman filter [7], Luenberger observer [8], model reference adaptive system [9], and sliding mode (SM) observer [10].

Most existing flux linkage observers, including that in [6], directly treat the flux linkage as the targeting observation goal and they are model-dependent. Nevertheless, it is difficult to always ensure the machine model is accurate in practice. One main reason is that the parameters (resistance and inductances) constructing the motor model are usually obtained before the motors leave the factories, but they are prone to mismatch with the real ones as the service period rises, magnetic saturation arises, and the working environment changes [14], [15]. In this case, the identified flux linkage from those observers is not reliable, reducing the demagnetization fault diagnosis precision. Now, the main solution to this issue is to improve the machine

Manuscript received 30 November 2022; revised 10 January 2023; accepted 11 February 2023. Date of publication 15 February 2023; date of current version 10 March 2023. *(Corresponding author: Chao Gong.)*

Yaofei Han and Shaofeng Chen are with the National Maglev Transportation Engineering R&D Center, Tongji University, Shanghai 200092, China (e-mail: ei_zx@tongji.edu.cn; shaofeng_chen@126.com).

Chao Gong and Yunwei Li are with the Department of Electrical and Computer Engineering, University of Alberta, Edmonton, AB T6G 2R3, Canada (e-mail: 1452101806@qq.com; yunwei.li@ualberta.ca).

Xing Zhao is with the School of Physics, Engineering and Technology, University of York, York YO10 5DD, U.K. (e-mail: xing.zhao@york.ac.uk).

Fanggang Zhang is with the Department of Mechanical Engineering, University of Birmingham, Birmingham B15 2TT, U.K. (e-mail: fxz625@student.bham.ac.uk).

Color versions of one or more figures in this article are available at https://doi.org/10.1109/TPEL.2023.3245052.

Digital Object Identifier 10.1109/TPEL.2023.3245052

model accuracy by using online resistance or inductance identification methods [16], but they seldom consider the inverse impact of PM demagnetization on the accuracy of resistance and inductance identification results. Hence, new flux linkage detection methods are highly required for the sake of accurate demagnetization detection.

This letter proposes an SM disturbance observer-based flux linkage detection scheme to diagnose the demagnetization fault for the IPM motors, which can avoid the impacts of resistance and inductance mismatch issue. The core technologies include motor modeling, overall disturbance observation, extraction of disturbance only caused by flux linkage mismatch, and flux linkage calculation for fault judgment. Compared with the existing flux linkage estimation strategies used for fault detection, the novelties of this letter can be summarized as follows:

1) Without constructing observers directly treating the flux linkage as the targeting observation goal, an SM disturbance observer is developed. Relying on the relationship between the flux linkage variations and the corresponding disturbances, the value of the flux linkage can be calculated. This is an indirect flux linkage observation method that has been seldom studied.
2) The disturbances caused by parameter mismatch are divided into two parts in this letter, that is, the disturbance caused by flux linkage and the disturbance caused by other parameters, such as resistance and inductances. To extract the disturbance corresponding to the flux linkage, a new current-analysis-based method is proposed based on the properties of the disturbances.
3) Because the resistance and inductance variations caused by the working environment and magnetic saturation are taken into account, their impacts on the flux linkage estimation results can be eliminated. This improves the accuracy of flux linkage identification and demagnetization fault diagnosis results, which is one of the main contributions of this letter. The effectiveness of the proposed method is verified by experiment.

II. IPM Motor Model With Disturbances Integrated

The q-axis electrical property of the IPM motor in the rotating reference frame can be described as

$$\frac{\mathrm{d}i_q}{\mathrm{d}t} = -\frac{R_s}{L_q}i_q - \frac{L_d}{L_q}p\omega_m i_d - \frac{\psi_f}{L_q}p\omega_m + \frac{u_q}{L_q} \tag{1}$$

where i_d and i_q are stator d- and q-axis currents, respectively. ω_m is angular speed, u_q is q-axis control voltage, p is the number of pole pairs, and L_d, L_q, R_s, and ψ_f are the real d-axis inductance, q-axis inductance, resistance, and flux linkage generated by PMs, respectively.

However, the measured inductances, resistance, and flux linkage (denoted as L_{d_m}, L_{q_m}, R_{s_m}, and ψ_{f_m}, respectively) need to be substituted into (1) for modeling practically, which are inclined to mismatch with the real parameters. In this case, there exist errors between the measured parameter values and the real ones, that is

$$\begin{cases} L_{d\_m} = \Delta L_d + L_d, L_{q\_m} = \Delta L_q + L_q \\ R_{s\_m} = \Delta R_s + R_s, \psi_{f\_m} = \Delta\psi_f + \psi_f \end{cases} \tag{2}$$

where ΔL_d and ΔL_q are d-axis and q-axis inductance errors arising from magnetic saturation and long service period, respectively. ΔR_s and $\Delta\psi_f$ are resistance and flux linkage errors, respectively. The parameter errors will further bring about disturbances for the motor model. Specifically, after substituting (2) into (1), the motor model with disturbances integrated can be derived as

$$\begin{cases} \frac{\mathrm{d}i_q}{\mathrm{d}t} = -\frac{R_{s\_m}}{L_{q\_m}}i_q - \frac{L_{d\_m}}{L_{q\_m}}p\omega_m i_d - \frac{\psi_{f\_m}}{L_{q\_m}}p\omega_m + \frac{u_q}{L_{q\_m}} + \frac{d\_\mathrm{all}}{L_{q\_m}} \\ d\_\mathrm{all} = d\_\mathrm{fl} + d\_el, d\_\mathrm{fl} = \Delta\psi_f p\omega_m \\ d\_\mathrm{el} = \Delta R_s i_q + \Delta L_d p\omega_m i_d + \Delta L_q \frac{\mathrm{d}i_q}{\mathrm{d}t} \end{cases} \tag{3}$$

where d_all is overall disturbance caused by all of the measured parameter values, and d_fl and d_el are the disturbances caused only by flux linkage and other parameters, respectively.

Based on (3), if the error d_fl can be identified, $\Delta\psi_f$ can be calculated using (4), which can be then adopted to calculate the real flux linkage using (2) for demagnetization fault judgment, whereas it is hard to distinguish d_fl and d_el from each other, leading to the fact that there is no one observer that can only detect d_fl without considering d_el. Now, a new issue of how to obtain the specific error caused by flux linkage mismatch arises, and the solution is the prerequisite of a disturbance observer-based demagnetization fault diagnosis strategy

$$\Delta\psi_f = \frac{d\_\mathrm{fl}}{p\omega_m}. \tag{4}$$

III. Proposed SM Disturbance Observer-Based Demagnetization Fault Diagnosis

Although d_fl cannot be identified by an observer, the overall disturbance d_all which is a state variable in (3) can be. Hence, this part develops an SM observer that has fast response to identify it first. Then, a current-analysis-based scheme is employed to extract d_fl from the overall disturbance. Finally, the flux linkage is calculated to diagnose the demagnetization fault and demagnetization degree.

A. SM Disturbance Observer

1) Structure of SM Disturbance Observer: Based on the SM variable structure theory, the structure of an SM disturbance observer derived from the machine model (3) can be described as

$$\frac{\mathrm{d}i_q^*}{\mathrm{d}t} = -\frac{R_{s\_m}}{L_{q\_m}}i_q^* - \frac{L_{d\_m}}{L_{q\_m}}p\omega_m i_d - \frac{\psi_{f\_m}}{L_{q\_m}}p\omega_m + \frac{u_q}{L_{q\_m}} + \frac{\lambda F(\overline{i_q})}{L_{q\_m}} \tag{5}$$

where $i_q{}^*$ is estimated current; λ is gain coefficient of the observer; and $\overline{i_q}$ and $F(\overline{i_q})$ are the error between the estimated current and the real one, and switching function, respectively

$$\overline{i_q} = i_q^* - i_q, F(\overline{i_q}) = \begin{cases} 1, & \text{if } \overline{i_q} \geq 0 \\ -1, & \text{if } \overline{i_q}, < 0. \end{cases} \tag{6}$$

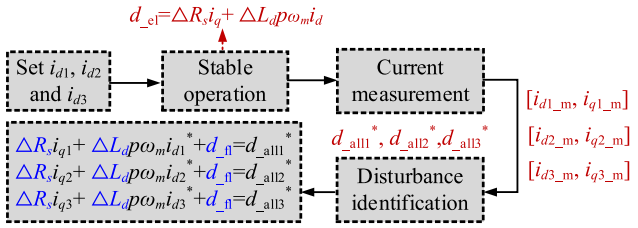

Fig. 1. Implementation of proposed disturbance extraction method.

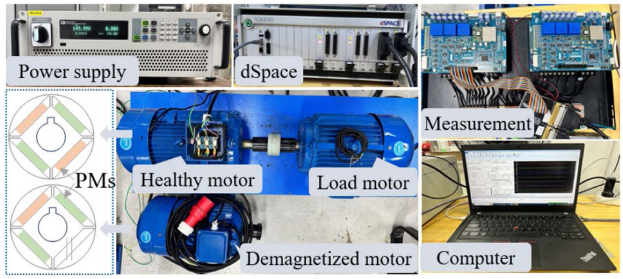

Fig. 2. Experimental test bench used for verifications.

When the observer reaches the equilibrium state, the overall disturbance $d_{\_all}^*$ can be estimated by

$$d_{\_all}^* = \lambda F(\overline{i_q}). \tag{7}$$

2) Stability Analysis: To analyze the stability of the proposed SM observer, the Lyapunov function requires to be established. To achieve the goal, a sliding surface s should be defined as

$$s = \overline{i_q}. \tag{8}$$

Then, the Lyapunov function V is

$$V = \frac{1}{2}s^2 = \frac{1}{2}\overline{i_q}^2. \tag{9}$$

From (9), it can be seen that $V > 0$, which is one essential condition making the observer stable. Now, we can conclude that the observer can work stably as long as the following condition can be satisfied:

$$\frac{\mathrm{d}V}{\mathrm{d}t} = \frac{\mathrm{d}\overline{i_q}}{\mathrm{d}t}\overline{i_q} = \underbrace{-\frac{R_{s\_}}{L_{q\_m}}\overline{i_q}^2}_{\text{part1}} + \underbrace{\frac{(\lambda F(\overline{i_q}) - d_{\_all})\overline{i_q}}{L_{q\_m}}}_{\text{part2}} < 0. \tag{10}$$

Because part1 in (10) is less than zero constantly, the equation can be simplified as

$$(\lambda F(\overline{i_q}) - d_{\_all})\overline{i_q} < 0. \tag{11}$$

When considering the sign of $\overline{i_q}$, (11) can be deduced as

$$\begin{cases} \lambda - d_{\_all} < 0, if\, \overline{i_q} \geq 0 \\ -\lambda - d_{\_all} > 0, if\, \overline{i_q} < 0 \end{cases} \rightarrow \lambda < -|d_{\_all}|. \tag{12}$$

To ensure the disturbance observer is stable, λ should be negative and its magnitude should be larger than the maximum disturbance. As for an IPM motor drive with finite overall disturbance, there must be a constant satisfying (12), and λ can be designed using the cut-and-trial method in practice.

B. Current-Analysis-Based Disturbance Extraction

By carefully looking at (3), two important features need to be addressed. First, when either the d-axis current or the q-axis one changes, $d_{\_el}$ will be different while $d_{\_fl}$ remains constant. Second, when the motor works stably, the differential term $\mathrm{d}i_q/\mathrm{d}t$ contained in $d_{\_el}$ equals zero. On these grounds, the disturbance caused by flux linkage mismatch can be extracted, of which implementation is shown in Fig. 1.

When the IPM motor rotates at the speed of ω_m stably, if the flux linkage detection request occurs, first, three different values are set as the d-axis reference currents (i_{d1}, i_{d2}, and i_{d3}) one by one. When the motor gets stable, $d_{\_el}$ in (3) can be simplified as (13), both the d- and q-axis currents are measured. And three sets of different currents will be obtained, that is, $[i_{d1\_m}, i_{q1\_m}]$, $[i_{d2\_m}, i_{q2\_m}]$, and $[i_{d3\_m}, i_{q3\_m}]$. It deserves to be mentioned that, first the reference and measured d-axis currents are theoretically equal. Second, the q-axis currents i_{q1}, i_{q2}, and i_{q3} are different because of the coupling effect and IPM motor load property [17]

$$d_{\_el} = \Delta R_s i_q + \Delta L_d p\omega_m i_d. \tag{13}$$

Then, the measured currents together with speed are substituted into the SM disturbance observer (5) to calculate the overall disturbances, which are $d_{\_all1}^*$, $d_{\_all2}^*$, and $d_{\_all3}^*$. Considering that current variations do not change $d_{\_fl}$, a system of equations with three unknowns (ΔL_d, ΔR_s, and $d_{\_fl}^*$) can be obtained

$$\begin{cases} \Delta R_s i_{q1\_m} + \Delta L_d p\omega_m i_{d1\_m} + d_{\_fl}^* = d_{\_all1}^* \\ \Delta R_s i_{q2\_m} + \Delta L_d p\omega_m i_{d2\_m} + d_{\_fl}^* = d_{\_all2}^* \\ \Delta R_s i_{q3\_m} + \Delta L_d p\omega_m i_{d3\_m} + d_{\_fl}^* = d_{\_all3}^* \end{cases} \tag{14}$$

where $d_{\_fl}^*$ is the disturbance to be calculated. Finally, by solving (14), the disturbance caused by flux linkage mismatch can be calculated

$$\begin{cases} d_{\_fl}^* = \frac{k_1 d_{\_all1}^* + k_2 d_{\_all2}^* + k_3 d_{\_all3}^*}{k_1+k_2+k_3} \\ k_1 = i_{d2\_m} i_{q3\_m} - i_{d3\_m} i_{q2\_m} \\ k_2 = i_{d3\_m} i_{q1\_m} - i_{d1\_m} i_{q3\_m} \\ k_3 = i_{d1\_m} i_{q2\_m} - i_{d2\_m} i_{q1\_m}. \end{cases} \tag{15}$$

C. Demagnetization Fault Diagnosis

After extracting $d_{\_fl}^*$ from the overall disturbance, it together with the motor speed can be substituted into (4) to calculate the flux linkage error first. Then, the real-time flux linkage can be obtained based on (2). Denote ψ_{f_m} as the initial flux linkage of the healthy motor, and if it is larger than the estimated value, the demagnetization fault occurs, and the demagnetization degree γ can be described as

$$\gamma = \frac{d_{\_fl}^*}{p\omega_m \psi_{f\_m}} \times 100\%. \tag{16}$$

IV. Verification Results

To validate the proposed SM disturbance observer-based demagnetization fault diagnosis strategy, experiment is conducted on two IPM motors (Fig. 2). One motor is healthy, which can simulate the uniform demagnetization fault. The other has the

TABLE I
PARAMETERS OF HEALTHY MOTOR

Parameter	Value	Unit
Measured stator winding resistance R_{s_m}	0.605	Ω
Measured d-axis inductance L_{d_m}	12.65	mH
Measured q-axis inductance L_{q_m}	13.5	mH
The number of pole pairs p	2	—
Measured flux linkage ψ_{f_m}	0.6873	Wb

same structure as the healthy motor, but one out of four PMs is removed, simulating the partial demagnetization fault. The parameters of the healthy motor are accurately measured by the authenticated offline methods, which are given in Table I, and without considering magnetic saturation and thermal variations, etc., the parameters in Table I can be treated as the accurate ones. The gain coefficient of the observer is set as -100 empirically. The dc-bus voltage is 150 V. The proposed algorithms are implemented on a dSPACE control board, and data are recorded by the dSPACE Control Desk. One motor working under the torque control mode is coupled to the test IPM motors to provide the required load. For the sake of comparison, apart from the offline-tested flux linkage values, the estimation results of a traditional magnetic flux estimation method in [16] are presented. Before illustrating the experimental results, it needs to be mentioned that first, the motor speed is 21 rad/s. Second, the load is 3 Nm. Third, considering that the practical overall disturbances may be caused by not only parameter mismatch but also other factors such as the nonlinearity of the inverter, compensation is employed in the experiment even if the phenomenon is not severe. Fourth, to obtain the disturbances $d^*_{\_all1}$, $d^*_{\_all2}$, and $d^*_{\_all3}$, the d-axis current is set as -2, 1, and 4 A, respectively. Third, when implementing the traditional flux estimation method, the d-axis current is set as -2 A.

A. Uniform Demagnetization

As long as the proposed method can accurately detect the flux linkage of the healthy motor regardless of the parameter mismatch issue, it must be able to diagnose the uniform demagnetization fault because the uniformly demagnetized motor has similar magnetic properties to the healthy one [13].

Without resistance and inductance mismatch, Fig. 3(a) and (b) show the motor performance and the overall disturbances $d^*_{\_all1}$, $d^*_{\_all2}$, and $d^*_{\_all3}$ estimated by the proposed technique. Based on these results, Fig. 3(d) presents the calculated flux linkage and the demagnetization fault diagnosis result, which are compared with the results obtained from the offline and traditional estimation methods. First, the estimated flux linkage using the proposed method is 0.6989 Wb, which is slightly higher than the offline-tested value. In this case, the demagnetization degree is -1.7%. Second, the traditional observer has high estimation accuracy as well, and the estimation result is 0.68 Wb, which is 1.1% lower than the offline tested value.

When considering the parameter mismatch issue, Fig. 4 shows the system performance and the flux linkage calculation results when the values of d-axis inductance, q-axis inductance, and resistance are assumed to be fourfold, twice and twice those in

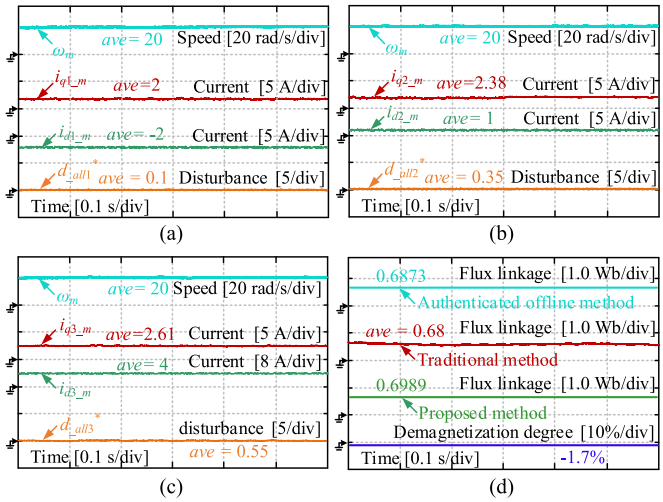

Fig. 3. Experimental results uniform demagnetization fault with matched resistance and inductances. (a) Results when d-axis current is -2 A. (b) Results when d-axis current is 1 A. (c) Results when d-axis current is 4 A. (d) Comparative flux linkage estimation results.

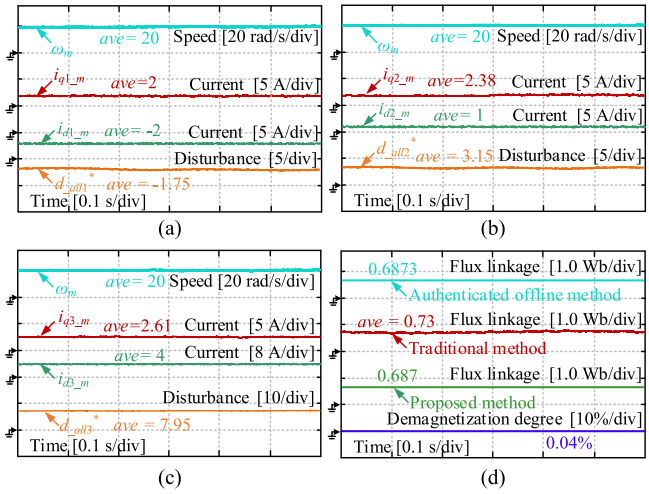

Fig. 4. Experimental results of uniform demagnetization fault with mismatched resistance and inductances. (a) Results when d-axis current is -2 A. (b) Results when d-axis current is 1 A. (c) Results when d-axis current is 4 A. (d) Comparative flux linkage estimation results.

Table I, respectively. Being different from the results in Fig. 3, the estimated flux linkage of the traditional observer is 0.73 Wb, which is 6.2% higher than the offline value. However, the proposed method shows higher estimation accuracy, of which result is 0.687 Wb.

B. Partial Demagnetization

As for the demagnetized motor, due to the change of its magnetic properties, the stator inductances cannot be consistent with those in Table I. But in the experiment, the inductance values of the healthy motor are used to construct the observers. In addition, to further reflect the characteristics of the proposed fault diagnosis method, the resistance value inside the observers is set as twice that in Table I. Fig. 5 shows the system performance when the partial demagnetization fault occurs. Compared

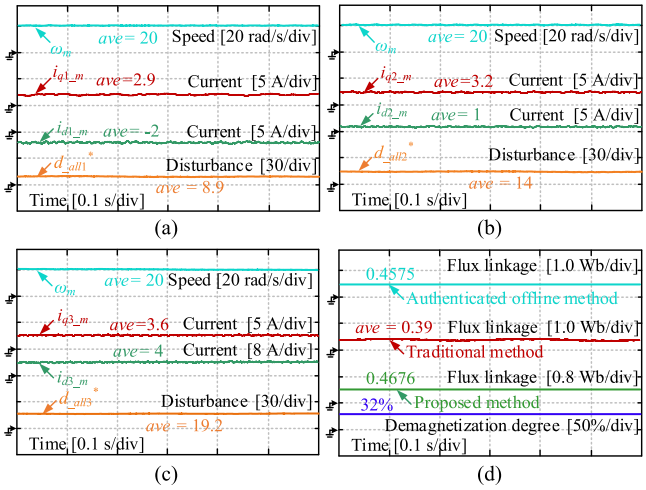

Fig. 5. Experimental results of partial demagnetization fault. (a) Results when d-axis current is -2 A. (b) Results when d-axis current is 1 A. (c) Results when d-axis current is 4 A. (d) Comparative flux linkage estimation results.

to the traditional flux linkage estimation method, the proposed one is closer to the offline-tested value, and the demagnetization degree of the IPM motor is about 32%.

V. Conclusion

This letter proposes a precise SM disturbance observer-based demagnetization fault diagnosis method for the IPM motors, avoiding the impacts of the resistance and inductance mismatch phenomena. The method is an extension of the flux linkage observation-based fault detection method introduced in patent US20120074879 A. The main contributions of this letter are as follows. First, the relationship between the distances and parameter mismatch is reflected through theoretical analysis. On this basis, a disturbance observation based method is developed to obtain the real-time flux linkage. Second, the disturbance caused only by the flux linkage variations is extracted from the overall disturabces which can be detected by the proposed SM observer. Finally, experimental results prove that the proposed method has high flux linkage estimation and demagnetization fault diagnosis accuracy.

References

[1] N. Zhao, G. Wang, D. Xu, L. Zhu, G. Zhang, and J. Huo, "Inverter power control based on DC-link voltage regulation for IPMSM drives without electrolytic capacitors," *IEEE Trans. Power Electron.*, vol. 33, no. 1, pp. 558–571, Jan. 2018.

[2] C. Gan, X. Li, Z. Yu, K. Ni, S. Wang, and R. Qu, "Modular seven-leg switched reluctance motor drive with flexible winding configuration and fault-tolerant capability," *IEEE Trans. Transp. Electrific.*, to be published, doi: 10.1109/TTE.2022.3225228.

[3] H. Chen, C. Gao, J. Si, Y. Nie, and Y. Hu, "A novel method for diagnosing demagnetization fault in PMSM using toroidal-yoke-type search coil," *Trans. Instrum. Meas.*, vol. 71, 2022, Art. no. 7501012.

[4] C. Desai and P. Pillay, "Back EMF, torque–angle, and core loss characterization of a variable-flux permanent-magnet machine," *IEEE Trans. Transp. Electrific.*, vol. 5, no. 2, pp. 371–384, Jun. 2019.

[5] J. Urresty, J. Riba, and L. Romeral, "Influence of the stator windings configuration in the currents and zero-sequence voltage harmonics in permanent magnet synchronous motors with demagnetization faults," *IEEE Trans. Magn.*, vol. 49, no. 8, pp. 4885–4893, Aug. 2013.

[6] B. Fahimi and A. Khoobroo, "Methods and apparatuses for fault management in permanent magnet synchronous machines using the field reconstruction method," U.S. Patent US20120074879 A1, 2012.

[7] Z. Yin, G. Li, Y. Zhang, J. Liu, X. Sun, and Y. Zhong, "A speed and flux observer of induction motor based on extended Kalman filter and Markov chain," *IEEE Trans. Power Electron.*, vol. 32, no. 9, pp. 7096–7117, Sep. 2017.

[8] J. Lai, C. Zhou, J. Su, M. Xie, J. Liu, and T. Xie, "A permanent magnet flux linkage estimation method based on luenberger observer for permanent magnet synchronous motor," in *Proc. 22nd Int. Conf. Elect. Mach. Syst.*, 2019, pp. 1–6.

[9] F. C. Dezza, G. Foglia, M. F. Iacchetti, and R. Perini, "An MRAS observer for sensorless DFIM drives with direct estimation of the torque and flux rotor current components," *IEEE Trans. Power Electron.*, vol. 27, no. 5, pp. 2576–2584, May 2012.

[10] S. Huang, G. Wu, F. Rong, C. Zhang, S. Huang, and Q. Wu, "Novel predictive stator flux control techniques for PMSM drives," *IEEE Trans. Power Electron.*, vol. 34, no. 9, pp. 8916–8929, Sep. 2019.

[11] M. Zhu, W. Hu, and N. C. Kar, "Acoustic noise-based uniform permanent-magnet demagnetization detection in SPMSM for high-performance PMSM drive," *IEEE Trans. Transp. Electrific.*, vol. 4, no. 1, pp. 303–313, Mar. 2018.

[12] D. W. Kang, "Analysis of vibration and performance considering demagnetization phenomenon of the interior permanent magnet motor," *IEEE Trans Magn* ., vol. 53, no. 11, Nov. 2017, Art. no. 8210807.

[13] J. Faiz and E. Mazaheri-Tehrani, "Demagnetization modeling and fault diagnosing techniques in permanent magnet machines under stationary and nonstationary conditions: An overview," *IEEE Trans. Ind. Appl.*, vol. 53, no. 3, pp. 2772–2785, May/Jun. 2017.

[14] B. Stumberger, G. Stumberger, D. Dolinar, A. Hamler, and M. Trlep, "Evaluation of saturation and cross-magnetization effects in interior permanent-magnet synchronous motor," *IEEE Trans. Ind. Appl.*, vol. 39, no. 5, pp. 1264–1271, Sep./Oct. 2003.

[15] J. Zhang, X. Wen, Y. Wang, and W. Li, "Modeling and analysis of nonlinear interior permanent magnet synchronous motors considering saturation and cross-magnetization effects," in *Proc. IEEE Transp. Electrific. Conf. Expo, Asia-Pacific*, 2016, pp. 611–615.

[16] Y. Han, C. Gong, G. Chen, Z. Ma, and S. Chen, "Robust MTPA control for novel EV-WFSMs based on pure SM observer based multistep inductance identification strategy," *IEEE Trans. Ind Electron.*, vol. 69, no. 12, pp. 12390–12401, Dec. 2022.

[17] C. Gong, Y. Hu, J. Gao, Y. Wang, and L. Yan, "An improved delay-suppressed sliding-mode observer for sensorless vector-controlled PMSM," *IEEE Trans. Ind Electron.*, vol. 67, no. 7, pp. 5913–5923, Jul. 2020.